ACS APPLIED MATERIALS & INTERFACES

Research Article

www.acsami.org

Stretchable Conductive Polypyrrole/Polyurethane (PPy/PU) Strain Sensor with Netlike Microcracks for Human Breath Detection

Mufang Li, Haiying Li, Weibing Zhong, Qinghua Zhao, and Dong Wang*

College of Materials Science and Engineering, Wuhan Textile University, Wuhan, 430200, China

ABSTRACT: The development of wearable electronics that can monitor human physiological information demands specially structured materials with excellent stretchability and electrical conductivity. In this study, a new stretchable conductive polypyrrole/polyurethane (PPy/PU) elastomer was designed and prepared by surface diffusion and in situ polymerization of PPy inside and on porous PU substrates. The structures allowed the formation of netlike microcracks under stretching. The netlike microcrack structures make possible the reversible changes in the electrical resistance of PPy/PU elastomers under stretching and releasing cycles. The variations in morphology and chemical structures, stretchability, and conductivity as well as the sensitivity of resistance change under stretching cycles were investigated. The mechanism of reversible conductivity of the PPy/PU elastomer was proposed. This property was then used to construct a waistband-like human breath detector. The results demonstrated its potential as a strain sensor for human health care applications by showing reversible resistance changes in the repeated stretching and contracting motion when human breathes in and out.

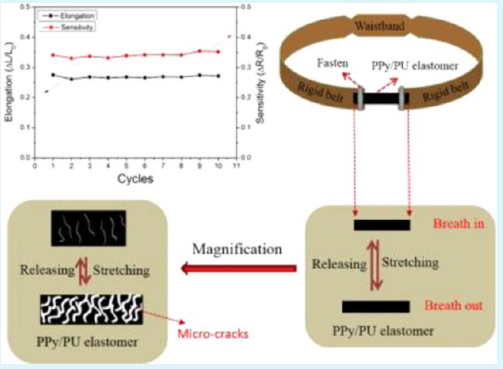

KEYWORDS: *stretchable conductive PPy/PU elastomer, netlike microcrack structure, stretching strain sensor, human breath detection, porous PU substrate, reversible change in electrical resistance*

1. INTRODUCTION

With the development of electronic devices moving toward being more integrated, portable, and intelligent, stretchable electric materials possessing both excellent flexibility and conductivity to cover arbitrary surfaces and movable parts have been the emerging and promising trend.[1−5] Stretchability will remarkably expand the applications of electronics, particularly for soft, wearable, and human-friendly sensors utilized in detecting human motion, breath, and pulse and monitoring personal health and therapeutics.[6−9] Among all the parameters of stretchable electric materials, stretchability, conductivity, and sensitivity are three key factors determining the performance of future sensors.[10−12]

Plenty of attempts have been made to enhance the performances of stretchable electric materials. Most widely employed strategies in attempting to prepare stretchable electric materials are development of new kinds of elastomers and design of new structures from currently available materials, such as the making of transformable conductive fibers and sheets,[13−15] combining of nanotube, graphene, and other electrical components with elastomers,[16−20] and embedding of different electric patterns into the elastomeric substrates[21−23] and other microstructure designs.[24,25] The largest difficulties, however, are to control and balance the stretchability, conductivity, and sensitivity of these materials.

We previously reported the fabrication of stretchable conductive polyurethane (PU) elastomer in situ polymerized with multiwalled carbon nanotubes (MWNTs) and its application for pressure sensor electrodes.[26] But the limitations in incorporating more MWNTs in PU chains make it hard to further improve the stretchability and electrical conductivity of PU/MWNTs elastomers. There are some early reports on the preparation of conductive PPy/PU composite foams by exposing the PU/oxidant foam to pyrrole vapors for polymerization.[27−29] However, because of the concern about the rigidity of PPy, very few studies discussed the changes in conductivity and structures of PPy/PU composites and attempted to apply them into health monitoring fields.

In the present study, pyrrole (Py) monomers were diffused into the porous PU elastomer substrates and were in situ polymerized to prepare a stretchable electric material with a thin layer of polypyrrole (PPy) strongly anchored on PU surfaces. The morphology, chemical structures, and electrical conductivity of porous PU substrates and PPy/PU elastomers were investigated. When being stretched, the PU substrate deformed and a netlike microcrack structure of PPY layer could be generated. The changes in morphology and the conductivity of PPy/PU elastomers under different elongations were studied. The conductive mechanism of the PPy/PU elastomer during stretching and releasing cycles was proposed. The stretchable conductive PPy/PU elastomer was successfully

Received: November 24, 2013
Accepted: December 26, 2013
Published: December 26, 2013

   dx.doi.org/10.1021/am4053305 | ACS Appl. Mater. Interfaces 2014, 6, 1313−1319

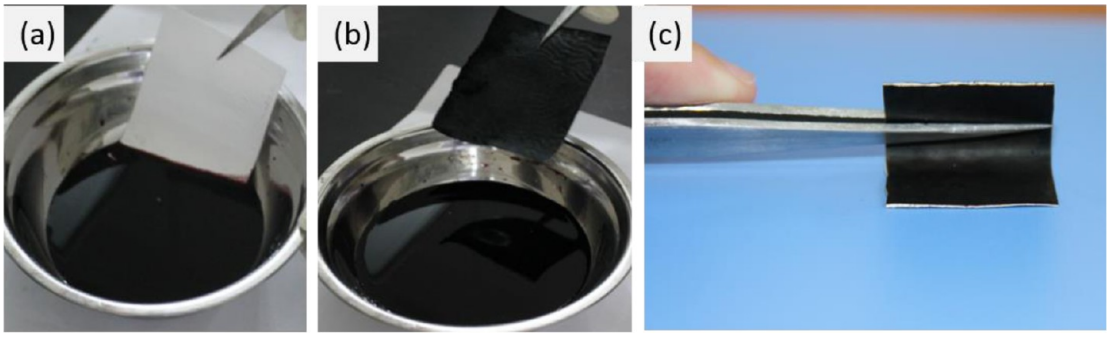

Figure 1. Photographs of (a) porous PU substrate before polymerization, (b) PPy/PU elastomer after surface in situ polymerization, and (c) surface and cross section of PPy/PU elastomer.

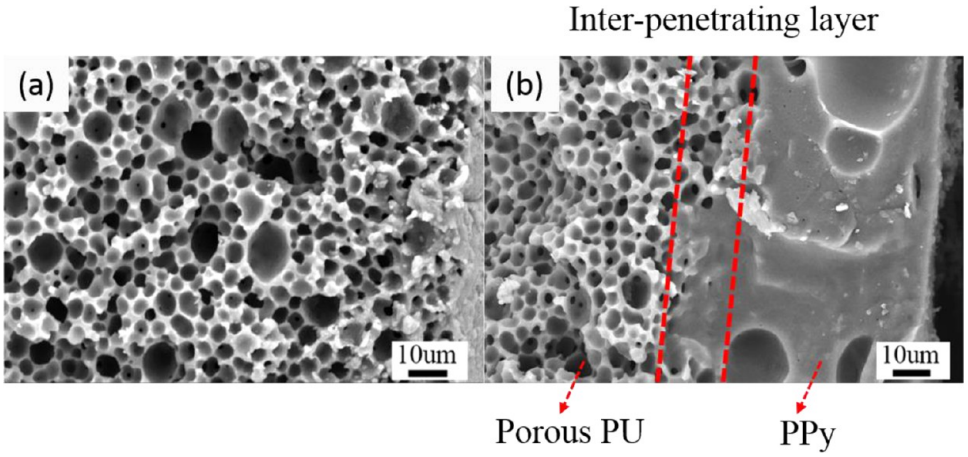

Figure 2. SEM images of fracture surface of (a) porous PU substrate and (b) PPy/PU elastomer.

employed to build a strain sensor for human breath detection with excellent sensitivity and repeatability.

2. EXPERIMENTAL SECTION

2.1. Materials. Polyurethane (PU) 2363-80AE pellets were purchased from Dow, U.S. 1-Methyl-2-pyrrolidinone (NMP), acetone (AC), *N*,*N*-dimethylformamide (DMF), pyyrole, 2-sulfosalicylic acid hydrate, and ferric nitrate were purchased from Sinoparm Chemical Reagent Co., Ltd. Anthraquinone-2-sulfonic acid sodium salt was supplied by Aladdin.

2.2. Preparation of Porous PU Substrates. The PU pellets were dissolved in DMF at 65 °C for 3 h. The pore generating agent of polyethylene glycol (PEG) was then added to the PU solution and mixed well. After that, the solutions were cast onto the PTFE plate to make the substrate and dried at the room temperature for 10 min. The substrate was then immersed into a solidification bath with 20 wt % of DMF in water for 10 min. The solidified PU substrates were then washed with the 80 °C hot water for 3 h and then dried in an oven at 65 °C overnight to prepare the porous polyurethane substrates.

2.3. Surface in Situ Polymerization of PPy/PU Elastomer. The bath ratio was defined as the weight of porous PU elastomer to that of the Py solution at a certain concentration. The PPy/PU elastomers were prepared with different bath ratios of 1:10, 1:30, 1:50, and 1:80. The detailed procedures were as follows. Anthraquinone-2-sulfonic acid sodium was dissolved in deionized water as doping agent. Aqueous ferric nitrate and 2-sulfosalicylic acid hydrate solution were used as oxidizing and stabilizing agent, respectively. First, the porous PU substrates were placed in a small beaker. Then the liquid pyrrole and sodium salt were added into the beaker with different bath ratios of 1:10, 1:30, 1:50, and 1:80 in an ice bath. Then the oxidant of iron salts was added in to the beaker gradually to make them mix very well and react for 12 h at an ice bath. The surface in situ polymerized PPy/PU substrates were then taken out and cleaned by water for some time until it was not rubbed off and then dried in the oven at 65 °C overnight. The prepared substrates were then cut into pieces for further tests.

2.4. Characterization. The chemical structures of PPy/PU were characterized by Fourier Transform infrared spectroscopy (FT-IR, Bruker Tensor 27). The morphologies of the pristine porous PU substrate and PPy/PU elastomer were analyzed using a scanning electron microscope (SEM, Hitachi X-650). The conductivity of the pristine porous PU substrate and PPy/PU elastomer were investigated at room temperature by a precision LCR meter (TH2818) and four-point-probe resistivity meter (RST-8). The stretching test was performed with the Instron 5566 at a rate of 5 mm/min.

3. RESULTS AND DISCUSSION

3.1. Morphology of Porous PU Substrate and PPy/PU Elastomer. To illustrate the in situ polymerization of Py on porous PU substrate, Figure 1 shows the photographs of porous PU substrate before and after Py in situ polymerization. After the polymerization, the surfaces of PPy/PU elastomer were macroscopically flat and smooth. From the image of PPy/PU elastomers shown in Figure 1c, it can be seen that a black thin layer of PPy was formed on both side surfaces of porous PU substrate, and the PPy/PU elastomer showed good flexibility.

Figure 2 exhibits SEM images of fracture surfaces of porous PU substrate and in situ polymerized PPy/PU elastomer. A large amount of pores could be found in the PU substrate, as shown in Figure 2a. After the polymerization of Py, a PPy layer with the thickness of about 40 μm on and inside porous PU substrates can be observed in Figure 2b. Moreover, it should be noted that PPy layers penetrated inside the porous structures of PU substrate at interfaces between PU and PPy, forming an

dx.doi.org/10.1021/am4053305 | ACS Appl. Mater. Interfaces 2014, 6, 1313−1319

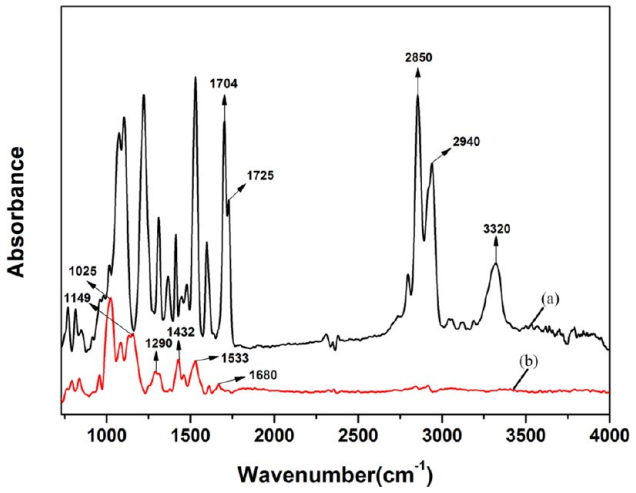

Figure 3. FTIR spectrum of (a) porous PU substrate and (b) PPy/PU elastomer.

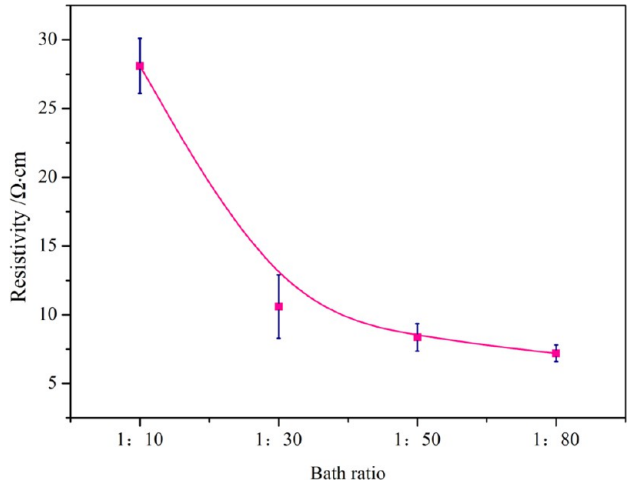

Figure 4. Effect of Py bath ratio on the electrical conductivity of PPy/PU elastomer.

interpenetrating layer with a thickness of about 10 μm near the surfaces of porous PU substrate. In the interpenetrating layer,

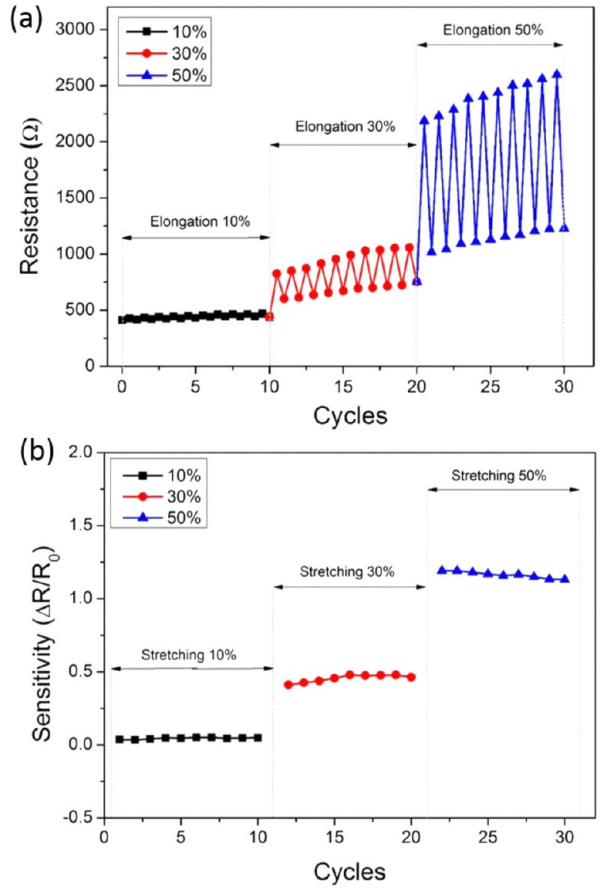

Figure 6. (a) Resistance as a function of stretching cycle numbers and (b) sensitivity of resistance change of PPy/PU elastomer with elongations of 10%, 30%, and 50%.

the pores of PU substrate were partially filled with the polymerized PPy. The large specific areas of porous PU substrate provide more chances for Py to diffuse inside and polymerize in the pores of PU substrate. This interpenetrating layer helps strengthen the interface adhesion between PU and PPy layers. The strong interface effectively prevented the falling off of the surface polymerized PPy layer from porous PU

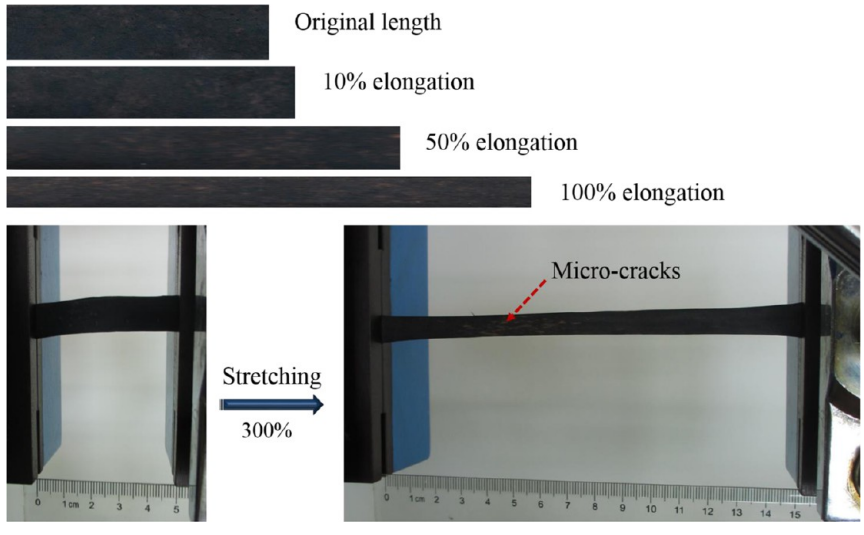

Figure 5. Stretchability of PPy/PU elastomer with various elongations.

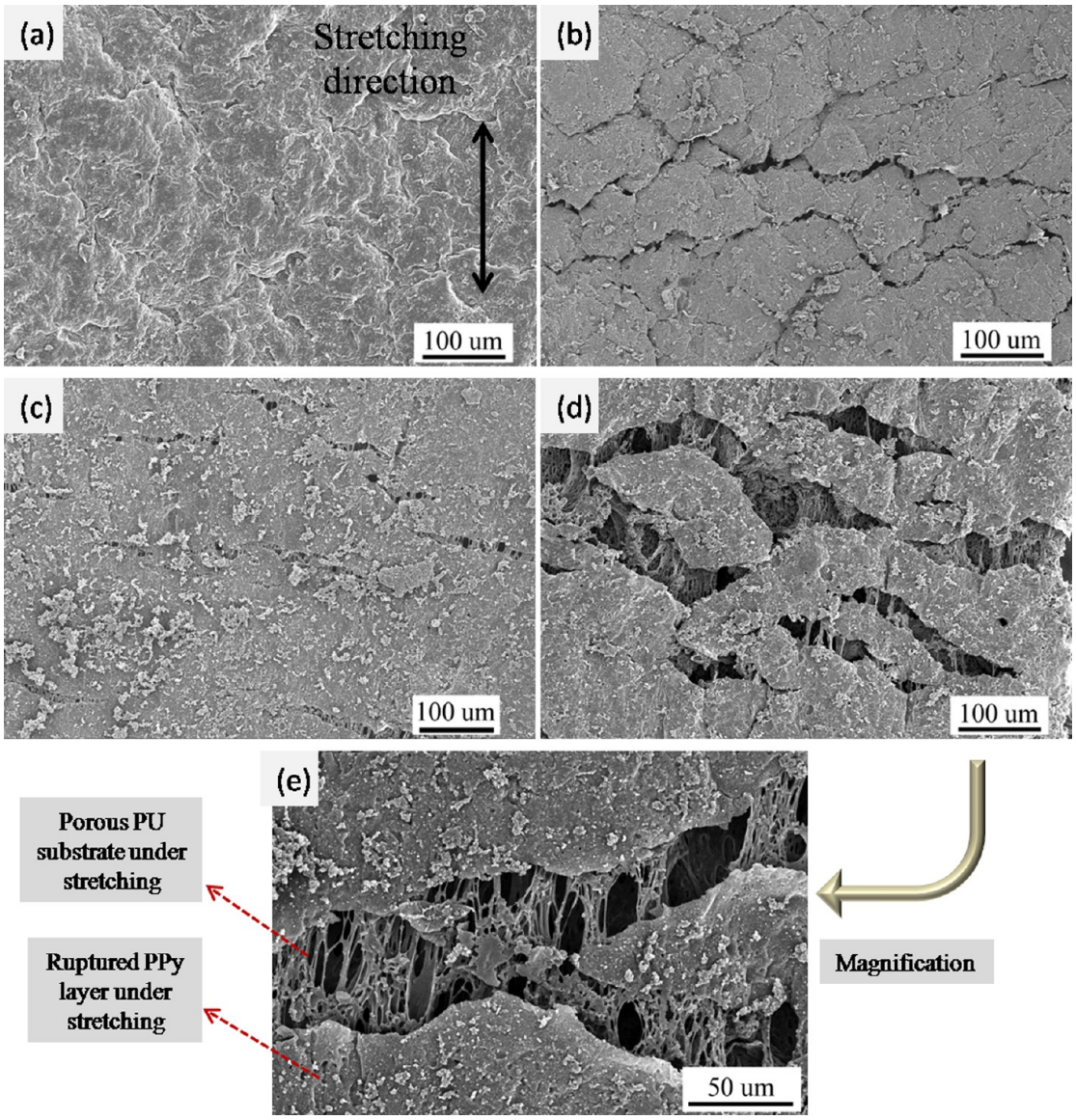

Figure 7. SEM images of PPy/PU elastomer under different elongation levels of (a) 0%, (b) 10%, (c) 30%, and (d) 50% and (e) magnification of (d).

substrate when PPy/PU elastomers were stretched and resulted in the occurrence of interconnected microcracks like nets in the PPy layer. The netlike cracks offered the possibility for the reversible change in electrical conductivity of PPy/PU elastomers during stretching and releasing cycles.

3.2. Chemical Structures of Porous PU Substrate and PPy/PU Elastomers. To demonstrate the chemical structures of porous PU substrate and the polymerized PPy layers on PU substrate, Figure 3 shows the FTIR spectrum of the porous PU substrate and PPy/PU elastomer. For pristine porous PU substrate, a strong absorption band appeared in the region of 2860−2940 cm^{-1} due to C−H symmetric/asymmetric stretching. Besides, two absorption bands were observed at 1704 and 1725 cm^{-1}, representing the hydrogen-bonded and free carbonyl groups.[29,30] The vibration band at 3320 cm^{-1} was assigned to the stretching modes of imido groups (−NH−) in urethane (−HNCOO−).[31] For the PPy/PU elastomer, the peaks at 1149 cm^{-1} were attributed to C−H in-plane deformation. The peaks at 1680 and 1290 cm^{-1} were due to the C═N and C−N bond stretching vibrations in the ring. The peak appearing at around 1025 cm^{-1} was attributed to the N−H in-plane bending vibration. The characteristic peaks at 1533 and 1432 cm^{-1} corresponded to the C═C stretching of pyrrole ring. The absorption peaks located at 792 and 837 cm^{-1} were attributed to C−H out-of-plane deformation. All of those characteristic peaks confirmed the formation of PPy on the surface of the porous PU substrate.[32−35]

3.3. Stretchable Conductivity of PPy/PU Elastomer. The added Py amount for in situ polymerization plays an important role in determining the electrical conductivity of PPy/PU elastomers. The bath ratio of PU porous elastomer weight to that of Py solution at a certain concentration varied from 1:10 to 1:80. The change in bath ratio from 1:10 to 1:80 indicated that more Py was used for polymerization. Figure 4 displays the effect of bath ratio on the electrical conductivity of PPy/PU elastomer. It can be found that the increase in the Py amount led to lower resistivity of PPy/PU elastomer. When the bath ratio reached 1:50, the conductivity leveled off. The resistivity of prepared PPy/PU elastomers with the bath ratio of 1:50 was 8.364 Ω·cm, demonstrating excellent conductivity.

dx.doi.org/10.1021/am4053305 | ACS Appl. Mater. Interfaces 2014, 6, 1313−1319

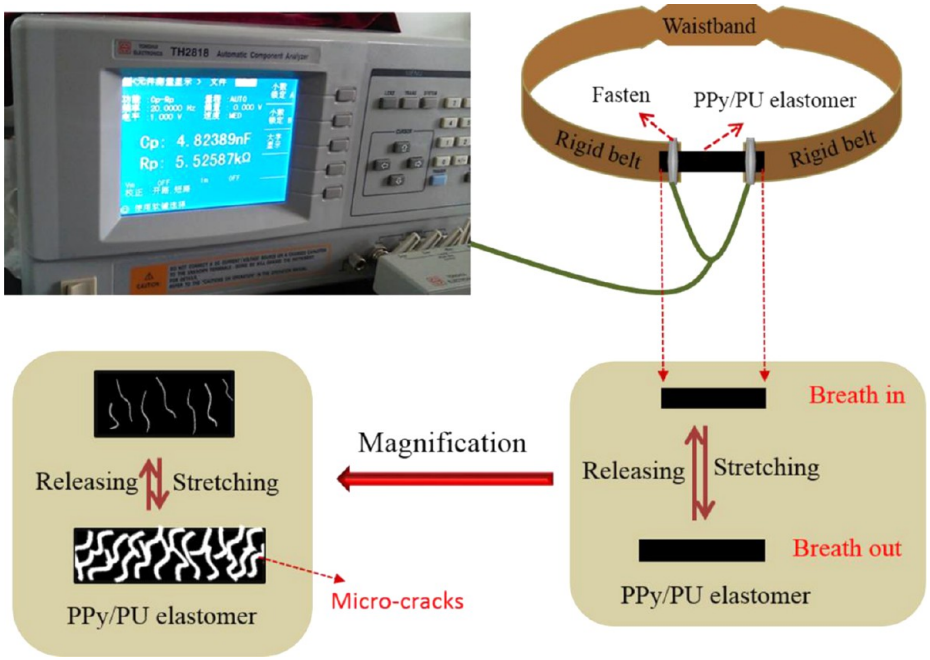

Figure 8. Schematic diagram of the waistband-like human breath detection sensor built from the PPy/PU elastomer.

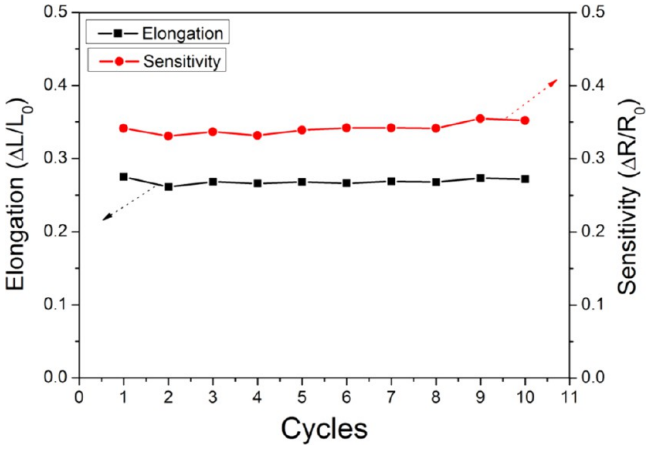

Figure 9. Elongation and sensitivity of the waistband-like human breath detection sensor.

Stretchability of PPy/PU elastomer is very important, since it has significant influence on the performance of strain sensors. Figure 5 shows a PPy/PU elastomer with different elongations. It could be seen that the there was no obvious mechanical damage for the PPy/PU elastomer when stretched to 300% of its original length. The netlike microcracks appeared on surfaces of PPy/PU elastomers. The density of microcracks increased with the elongations. The maximum elongation without the occurrence of significant fracture that PPy/PU elastomer could withstand was up to 420%. It is noted that no significant peeling off of the PPy layer was observed during stretching cycles.

To study the change in the electrical conductivity of PPy/PU elastomers during stretching and releasing cycles, the resistance variance of PPy/PU elastomers at different elongations of 10%, 30%, and 50% was measured under repeated stretching cycles and plotted in Figure 6a. The electrical conductivity is inversely proportional to the resistance. The sensitivity of resistance change of PPy/PU elastomers was characterized by the ratio of the difference in resistance (ΔR) after and before stretching to the one before stretching (R_0), as shown in Figure 6b. The resistance of PPy/PU elastomers increased when stretched but returned upon being released. It can be found that the resistance behavior of PPy/PU elastomer during the stretching and releasing cycle was different from that during the subsequent cycle. The resistance slightly went up with stretching and releasing cycles. Moreover, the sensitivity of resistance change of PPy/PU elastomer depended on the elongation levels. At the 10% elongation, the value of $\Delta R/R_0$ was 4.6%. The further increase in the elongations to 30% and 50% caused the sensitivity to climb to 44% and 116%, respectively.

To understand the electrically conductive mechanism of PPy/PU elastomer during stretching and releasing cycles, Figure 7 shows SEM images of PPy/PU elastomer when being stretched to different elongation levels. A compact PPy layer without microcracks stayed on surfaces of porous PU substrate with 0% elongation. Netlike microcracks appeared when the PPy/PU elastomer was stretched, as shown in Figure 7b–e. Narrow microcracks could be found at an elongation of 10%. The number of microcracks gradually increased with the elongation. Microcracks became wider with an increase in the elongation. As a result, the electrical resistance of PPy/PU elastomer was raised. Although microcracks grew with elongation, the PPy layer still tightly adhered to the deformed porous PU substrates and connected with each other, like a net. The generation of netlike microcracks under stretching may result from the fact that the porous structures randomly dissipated the applied stress and effectively transferred the dissipated stress to PPy layer through the strong interface adhesion. When the PPy/PU elastomer was released, the porous PU substrate relaxed and caused the shrinking of the microcrack in width, even closing. Therefore, the electrical resistance of PPy/PU elastomer decreased. At a smaller strain of 10%, the microcracks were few and smaller and the resistance change sensitivity was low. For larger elongations of 30% and 50%, more microcracks were introduced and the

dx.doi.org/10.1021/am4053305 | ACS Appl. Mater. Interfaces 2014, 6, 1313–1319

width became broader. The resistance increased sharply upon stretching; thus, the sensitivity significantly improved. Furthermore, the repeated elongations of 30% or 50% resulted in generation of partially irreversible microcracks, which causes the resistance of PPy/PU elastomers to be slightly raised when released. The property that resistance of PPy/PU elastomer could reversibly change with elongations makes it a potential candidate for the development of strain sensors.

3.4. Strain Sensor for Human Breath Detection from PPy/PU Elastomer. Figure 8 schematically illustrates the fabrication of a waistband-like strain sensor for human breath detection from the stretchable and conductive PPy/PU elastomers. The PPy/PU elastomer in the belt form was embedded inside the waistband and linked two ends of the rigid belt. The rigid belt without elastic deformation under stretching stress was used to minimize the effect of its own elasticity on the detection efficiency of strain sensor. The length and electrical resistance of the waistband changed when it was subjected to a repeated stretching and contracting motion during human breathing in and out. During breathing out, the elastic PPy/PU substrate was stretched, resulting in the increase in the electrical resistance of substrate. During breathing in, the stretched PPy/PU substrate relaxed and returned to its original length. As a result, the resistance decreased. The repeated reversible changes in the length and resistance were recorded to monitor the human breath. Figure 9 shows the elongations ($\Delta L/L_0$) and sensitivities ($\Delta R/R_0$) of the waistband-like human breath detector. The stretching strain of the waistband from breath-in to breath-out for an adult was less than 30%. The sensitivity of resistance change was up to 35%. In addition, the change in the length and resistance exhibited very little variation during ten breathing cycles. The results fit well with the data shown in Figure 6, which indicated good sensitivity and repeatability of the strain sensor from PPy/PU elastomers for human breath detection.

4. CONCLUSION

The stretchable conductive PPy/PU elastomers were prepared in this study. The SEM and FTIR results demonstrated that the Py was diffused inside the porous structures of PU substrates and that successful in situ polymerization occurred inside the pores and onto surfaces of PU substrates, forming a PPy/PU interpenetrating interface layers and PPy surface adsorption layers on PU substrates. The electrical resistivity of PPy/PU elastomer could reach 8.364 Ω·cm with a Py bath ratio of 1:50. The PPy/PU elastomer showed excellent stretchability with a maximum elongation of 420%. The reversible changes in the conductivity of PPy/PU elastomer during stretching and releasing cycles could be attributed to the formation of netlike microcracks on the porous PU substrate which was generated because of the strongly adhered PPy/PU interface layers. The sensitivity of the PPy/PU elastomer was enhanced significantly with elongations. The $\Delta R/R_0$ was 116% at an elongation of 50%. Furthermore, the PPy/PU elastomer was successfully employed to resemble a waistband-like strain sensor, which demonstrated excellent stretchability, sensitivity, and repeatability for human breath detection.

AUTHOR INFORMATION

Corresponding Author

*E-mail: wangdon08@126.com. Phone: +86-27-59367691.

Notes

The authors declare no competing financial interest.

ACKNOWLEDGMENTS

The authors are grateful for the financial support from National Nature Science Foundation (Grant 51273152), Program for New Century Excellent Talents in University (Grant NCET-12-0711), Hubei Province "Science Fund for Distinguished Young Scholars", and Wuhan "Chenguang" Schorship.

REFERENCES

(1) Zu, M.; Li, Q. W.; Wang, G. J.; Byun, J. H.; Chou, T. W. *Adv. Mater.* **2013**, *23*, 789−793.
(2) Stoyanov, H.; Kollosche, M.; Risse, S.; Waché, R.; Kofod, G. *Adv. Mater.* **2013**, *25*, 578−583.
(3) Bae, S. H.; Lee, Y.; Sharmaa, B. K.; Lee, H. J.; Kim, J. H.; Ahn, J. H. *Carbon* **2013**, *51*, 236−242.
(4) Lee, J.; Wu, J. A.; Ryu, J. H. *Small* **2012**, *8*, 1851−1856.
(5) Lee, J.; Wu, J. A.; Shi, M. X.; Yoon, J.; Park, S. I.; Li, M.; Liu, Z. J.; Huang, Y. G.; Rogers, J. A. *Adv. Mater.* **2011**, *23*, 986−991.
(6) Cheng, S.; Wu, Z. G. *Adv. Funct. Mater.* **2011**, *21*, 2282−2290.
(7) Lu, N. S.; Lu, C.; Yang, S. X.; Rogers, J. A. *Adv. Funct. Mater.* **2012**, *22*, 4044−4050.
(8) Yamada, T.; Hayamizu, Y.; Yamamoto, Y.; Yomogida, Y.; Izadi-Najafabadi, A.; Futaba, D. N.; Hata, K. *Nat. Nanotechnol.* **2011**, *6*, 296−301.
(9) Yun, D.; Yun, K. S. *Electron. Lett.* **2013**, *49*, 65−66.
(10) Ge, J.; Yao, H. B.; Wang, X.; Ye, Y. D.; Wang, J. L.; Wu, Z. Y.; Liu, J. W.; Fan, F. J; Gao, H. L.; Zhang, C. L.; Yu, S. H. *Angew. Chem., Int. Ed.* **2013**, *6*, 1654−1659.
(11) Hao, S. J.; Cui, L. S.; Chen, Z. H.; Jiang, D. Q.; Shao, Y.; Jiang, J.; Du, M. S.; Wang, Y. D.; Brown, D. E.; Ren, Y. *Adv. Funct. Mater.* **2013**, *25*, 1199−1202.
(12) Chen, M. T.; Tao, T.; Zhang, L.; Gao, W.; Li, C. Z. *Chem. Commun.* **2013**, *49*, 1612−1614.
(13) Sun, B.; Long, Y. Z.; Liu, S. L.; Huang, Y. Y.; Ma, J.; Zhang, H. D.; Shen, G. Z.; Xu, S. *Nanoscale* **2013**, *5*, 7041−7045.
(14) Xu, Z.; Liu, Z.; Sun, H. Y.; Gao, C. *Adv. Mater.* **2013**, *25*, 3249−3253.
(15) Shang, Y. Y.; He, X. D.; Li, Y. B.; Zhang, L. H.; Li, Z.; Ji, C. Y.; Shi, E. Z.; Li, P. X.; Zhu, K.; Peng, Q. Y.; Wang, C.; Zhang, X. J.; Wang, R. G.; Wei, J. Q.; Wang, K. L.; Zhu, H. W.; Wu, D. H.; Cao, A. Y. *Adv. Mater.* **2012**, *24*, 2896−2900.
(16) Ma, R.; Menamparambath, M. M.; Nikolaev, P.; Baik, S. *Adv. Mater.* **2013**, *25*, 2548−2553.
(17) Chun, K. Y.; Kim, S. H.; Shin, M. K.; Kim, Y. T.; Spinks, G. M.; Aliev, A. E.; Baughman, R. H.; Kim, S. J. *Nanotechnology* **2013**, *24*, 165401-1−165401-9.
(18) Li, X.; Zhang, R. J.; Yu, W. J.; Wang, K. L.; Wei, J. Q.; Wu, D. H.; Cao, A. Y.; Li, Z. H.; Cheng, Y.; Zheng, Q. S.; Ruoff, R. S.; Zhu, H. W. *Sci. Rep.* **2012**, *2*, 870-1−870-6.
(19) Hu, W. L.; Niu, X. F.; Li, L.; Yun, S. R.; Yu, Z. B.; Pei, Q. B. *Nanotechnology* **2012**, *23*, 344002-1−344002-9.
(20) Araki, T.; Nogi, M.; Suganuma, K.; Kogure, M.; Kirihara, O. *IEEE Electron Device Lett.* **2011**, *32*, 1424−1426.
(21) Park, M.; Im, J.; Shin, M.; Min, Y.; Park, J.; Cho, H.; Park, S.; Shim, M. B.; Jeon, S.; Chung, D. Y.; Bae, J.; Park, J.; Jeong, U.; Kim, K. *Nat. Nanotechnol.* **2012**, *7*, 803−809.
(22) Guo, R. S.; Yu, Y.; Xie, Z.; Liu, X. Q.; Zhou, X. C.; Gao, Y. F.; Liu, Z. L.; Zhou, F.; Yang, Y.; Zheng, Z. J. *Adv. Mater.* **2013**, *25*, 3343−3350.
(23) Moon, G. D.; Lim, G. H.; Song, J. H.; Shin, M.; Yu, T.; Lim, B.; Jeong, U. *Adv. Mater.* **2013**, *25*, 2707−2712.
(24) Pang, C.; Lee, G. Y.; Kim, T.; Kim, S. M.; Kim, H. N.; Ahn, S. H.; Suh, K. Y. *Nat. Mater.* **2012**, *11*, 795−801.
(25) Yao, H. B.; Ge, J.; Wang, C. F.; Wang, X.; Hu, W.; Zheng, Z. J.; Ni, Y.; Yu, S. H. *Adv. Mater.* **2013**, *25*, 6692−6698.

(26) Wang, D.; Li, H. Y.; Li, M. F.; Jiang, H. Q.; Xia, M.; Zhou, Z. *J. Mater. Chem. C* **2013**, *1*, 2744−2749.
(27) Wang, Y. B.; Sotzing, G. A.; Weiss, R. A. *Chem. Mater.* **2008**, *20*, 2574−2582.
(28) Njuguna, J.; Pielichowski, K. *J. Mater. Sci.* **2004**, *39*, 4081−4094.
(29) Kotal, M.; Srivastava, S. K.; Paramanik, B. *J. Phys. Chem. C* **2011**, *115*, 1496−1505.
(30) Yanilmaz, M.; Kalaoglu, F.; Karakas, H.; Sarac, A. S. *J. Appl. Polym. Sci.* **2012**, *125*, 4100−4108.
(31) Luo, Y. L.; Wang, B. X.; Xu, F. *Sens. Actuators, B* **2011**, *156*, 12−22.
(32) Mokrane, S.; Akhloufi, L. M.; Alonso-Vante, N. *J. Solid State Electrochem.* **2008**, *12*, 569−574.
(33) Chougule, M. A.; Pawar, S. G.; Godse, P. R.; Mulik, R. N.; Sen, S.; Patil, V. B. *Soft Nanosci. Lett.* **2011**, *1*, 6−10.
(34) Eisazadeh, H. *World J. Chem.* **2007**, *2*, 67−74.
(35) Gonzalez-Tejera, M. J.; de la Plaza, M. A.; Sanchez de la Blanca, E.; Hernandez-Fuentes, I. *Polym. Int.* **1993**, *31*, 45−50.